11th Australasian Fluid Mechanics Conference
University of Tasmania, Hobart, Australia
14-18 December 1992

TURBULENCE STATISTICS FROM A MULTI-FRAME PARTICLE TRACKING TECHNIQUE

M.F. HIBBERD

CSIRO Division of Atmospheric Research
Private Bag 1, Mordialloc, VIC 3195
AUSTRALIA

ABSTRACT

A wide variety of particle tracking techniques has been described in the literature over many years. Recently, interest in these *whole field* techniques (*cf.* point measurements) has been revived with the growing use of video recorders for data acquisition and computerization of analysis procedures. However, these methods are still usually restricted to fairly simple flows with analysis only providing details of the velocity field. Here we report on a multi-frame multi-particle tracking algorithm that has successfully been used to determine up to fourth-order velocity statistics for simulated data as well as in a turbulent convective boundary layer experiment.

INTRODUCTION

The last decade has seen a revival of interest in quantitative flow visualization techniques. This has been due in part to improvements in video technology and increased computerization of analysis, which allows direct digital image processing rather than requiring tedious manual processing of photographic images (Hesselink, 1988).

The range of techniques for determining velocities in flows seeded with tracer particles, broadly referred to as particle-imaging velocimetry (PIV) has recently been reviewed by Adrian (1991). At low particle densities, where the typical separation between images of individual particles in the image plane is much larger than the distance travelled by a particle between exposures, it is possible to devise methods for identifying and following individual particles from exposure to exposure. This is commonly termed particle tracking velocimetry (PTV) or low-image-density PIV. If the particle locations are recorded as a function of time on a single photograph, streak photographs are obtained. For quantitative analysis, it is more usual to use a sequence of exposures short enough to freeze the motion and record the results on movie film or video tape.

At higher particle densities, where the number of particles makes tracking of individual particles difficult as well as time consuming, one measures the displacement of small groups of particles by interrogating small areas of the image and using digital or optical correlation techniques (high-image-density PIV). If the concentration of scattering particles becomes so large that their images overlap in the image plane and the flow is illuminated with laser light, then the random phase differences between the images of the particles creates interference patterns known as laser speckle. For sufficiently small displacements and assuming negligible relative motion between the particles, the speckle pattern retains its character and the velocity can be determined by measuring the speckle displacement (laser-speckle velocimetry).

This paper is concerned with low seeding densities and describes a multi-frame particle tracking technique. In addition to determining velocity vectors, an important new feature has been to extend the analysis to the determination of higher order velocity moments (variance, skewness and kurtosis). Its performance has been checked using simulated data with known statistical properties before applying it to a turbulent convective boundary layer study.

PARTICLE TRACKING PROCEDURE

Data Acquisition

Standard video recordings of tracer particles illuminated with a sheet of laser or white light provide the initial data for the tracking algorithm described here. These video recordings are digitized using a Labtam computer fitted with an Imaging Technology IP512 frame grabbing system with 512x512 pixel resolution. A timebase corrector is used to avoid loss of video synchronization during the frame-grabbing procedure. Pre-processing by the IP512 histogram/feature-extraction module provides blanking and contrast enhancement and is adjusted to produce an intensity at each pixel of either 1 or 0, according to whether or not a particle is detected. By recording only the locations of the on-pixels, the real-time storage requirements are dramatically reduced compared to those for full frame details with a grey-scale intensity level at each pixel. Thus, rather than only being able to process several frames at a time, as is commonly the case, it is possible with this system to record the locations of several hundred particles over several hundred frames in a single file (limited only by available RAM). In the final preprocessing stage, the data are fed through a declustering routine that locates the centre of each group of lit pixels. An affine transformation based on calibration points in the flow is used to convert these locations to laboratory coordinates.

The multi-frame feature means that very low velocities can be accurately determined by tracking particles over many frames and/or sampling the video recording at less than 25Hz. The need to avoid track overlap between successive frames and the maximum framing rate of 25Hz sets an upper limit of about 10cm/s on the velocities that can be detected for typical laboratory experiments with a 50cm wide field of view. To ensure that only velocity components in the illumination plane are resolved, contributions from motion normal to this plane are minimized by illuminating the flow with a thin laser light sheet or maintaining a large distance from the illumination to image plane and using a telephoto lens on the video camera. Compared to *single*-frame multiple-exposure techniques, the time resolution of the particle trajectories in this *multi*-frame technique retains directional information and eliminates

problems arising from overlapping trajectories or particles entering or leaving the illuminated field of view during the recording.

Particle Tracking Algorithm

The tracking algorithm uses a nearest neighbour method with trajectory extrapolation. The analysis proceeds frame by frame. It requires input for the maximum expected velocity in the flow v_{max} and the maximum expected acceleration a_{max} over the timestep Δt between frames. For each particle not in a track (all particles in the first frame), the subsequent frame is searched for a nearest neighbour within a circle with radius equal to $v_{max}\Delta t$ and centred on its current location. For each particle already in a track, the current velocity is used to extrapolate to its anticipated location in the next frame and the search circle is centred on this location with a radius equal to $a_{max}(\Delta t)^2$. In both cases, the radius incorporates a factor to account for the digitization error from the video data. The output of this tracking algorithm is a set of time-resolved particle trajectories. Separate routines are used to analyse these trajectories to determine velocity vectors, draw streamlines or calculate higher-order moments.

Tracking particles over several frames greatly reduces the errors associated with simple nearest neighbour methods. Typically, only trajectories with a minimum track length of 3 are used in further analysis. The tracking algorithm also generates diagnostic statistics on the distribution of velocities and accelerations of tracked particles, which provides a check on the original choices of v_{max} and a_{max} and enables the input parameters to be modified for repeated or further analysis. Together with results on the distribution of separations of particles in the frame, these diagnostics provide feedback on the appropriateness of the seeding density of particles in the flow. Criteria for selecting the seeding density have been described by Adrian (1991).

The tracking algorithm is implemented on a DEC Microvax 2 and typically uses about 300s CPU time for analysis of 100 frames each containing 100 particles.

SIMULATED TEST DATA

The performance of the tracking algorithm, including the influence of uneven particle distribution and data dropouts (seen as *twinkling* in real data) as well as its reliability for determining higher-order statistics, was checked using a set of specially generated test data. In order to produce realistic particle trajectories for turbulent flows and in particular with statistics similar to those found in the convective boundary layer (described below), a Lagrangian particle model based on the Langevin equation was used (Hurley and Physick, 1992). The model parameterizations used in this implementation included homogeneous Gaussian turbulence for both horizontal components and inhomogeneous skewed turbulence for the vertical component.

This model (with timesteps of 0.002s) was used to generate 3-D trajectories for several hundred particles that were started at randomly distributed locations within a 3-D box. Any particles leaving the box were replaced by new particles to maintain a constant number of current trajectories. The maximum velocities were 3cm/s. Other details of the model are given in the reference above; the turbulence properties of the simulated field are shown below.

Each 0.2s, the horizontal and vertical components of the locations (x, z) and the velocities (u, w) of all particles (*ca.* 150) within a smaller region 60cm wide (X), 25cm high (Z), and 2cm thick (Y) were stored. This simulated the illumination of a 60cmx25cm field of view with a 2cm thick light sheet and allowed particles to enter and leave the field of view in a realistic manner. The model was run for a total of 200s to produce 1000 frames of data. An example of the particle trajectories recorded over a 20s period is shown in Fig. 1.

The velocity statistics of this simulated field were calculated from the stored velocity components. With the model assumption of horizontal homogeneity, the statistics were spatially averaged in the x-direction. For the horizontal velocity component $u(z)$, we calculated the mean value $\overline{u}(z)$, where the overbar denotes an ensemble average, and the fluctuating component $u'(z) = u(z) - \overline{u}(z)$, as well as the variance

$$\sigma_u^2 = \overline{u'^2}(z) ,$$

the skewness

$$S_u = \overline{u'^3}(z)/\sigma_u^3(z) ,$$

and the kurtosis

$$K_u = \overline{u'^4}(z)/\sigma_u^4(z) ,$$

with similar definitions for the vertical velocity component w. These central moments were calculated at each of 25 1cm wide levels in the vertical for the whole set of velocity components recorded over the 1000 frames; there were about 5000 values at each level. The results from these *true* data are shown as the solid lines in Figs. 2(a)-(d).

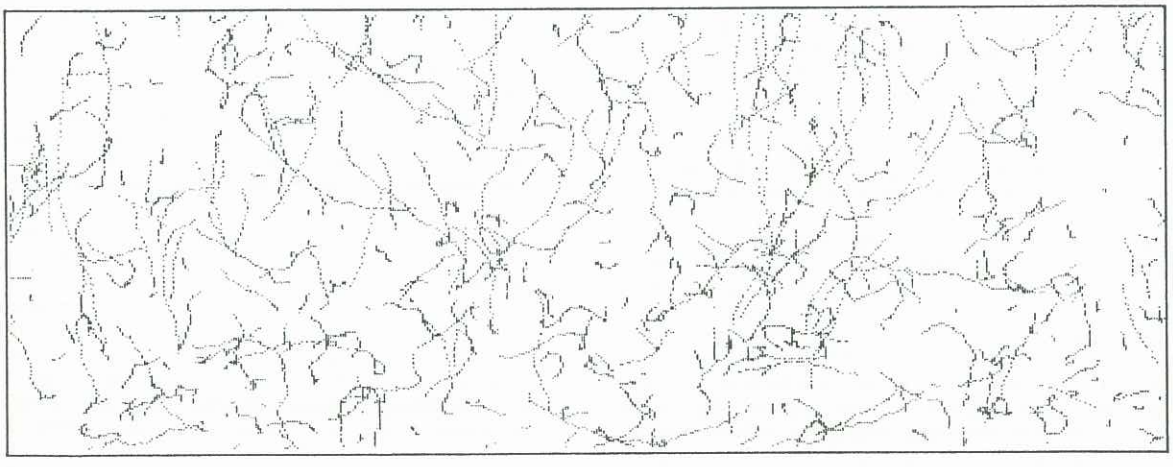

Fig. 1 Example of simulated particle trajectories in 60cmx25cm field of view. Overlay of 100 frames of data with timesteps of 0.2s.

Particle Tracking Results

Data equivalent to those obtained from video recordings were produced by using the particle locations recorded for the simulated data at each 0.2s timestep. To simulate the digitization error resulting from the limited resolution of video recorders, the x-values were *defocussed* to the closest 0.12cm step (= 60cm/512pixels) and the z-values to 0.08cm steps. The better resolution in the z-direction is due to the square 512x512 format of the frame grabber for a rectangular video image. Furthermore, to simulate *twinkling* that is observed when collecting real data (due to scattering intensities close to the video sensitivity limit or shadowing), a random selection of up to 10% of the particles in each frame was removed and the order in which the particles appear in the list for each frame was randomized.

Ten groups of 100 frames each were then analyzed using the particle tracking algorithm. The velocities of all particle trajectories with a minimum track length of 3 were estimated and the central moments calculated. The results are shown as the symbols (o, ■) in Figs. 2(a)-(d).

The mean velocities show good agreement with maximum differences of less than 0.01cm/s between the *true* data and the results from the tracking. (The non-zero values of $\overline{w}$ are an artifact in the simulation procedure.) There is also good agreement for the variances. The variances calculated from the tracked data are on average higher than the *true* values, by 0.014cm^2/s^2 for σ_u^2 and 0.008cm^2/s^2 for σ_w^2 but this is due to the contribution from the digitization error. In fact, it compares well with calculated values of 0.017 and 0.008 respectively, based on the known errors in determining particle displacements.

In contrast, the skewness is much noisier, even for the *true* data, but the difference between $S_u \approx 0$ and $S_w \approx 0.4$ can be clearly determined. The results suggest that it would be possible to distinguish differences in skewness of *ca.* 0.1 with this method. Similarly, the kurtosis ($K = 3$ for a Gaussian distribution) shows significant scatter in both the *true* and tracked data with $K_u \approx 3.0$ and $K_w \approx 2.5$. The good agreement between the *true* and tracked data indicate that in cases where sufficient sampling is possible, good measurements of turbulence statistics can be obtained from the analysis of velocities obtained from the particle tracking algorithm.

The application of the algorithm to a real laboratory flow is now described.

TURBULENT CONVECTIVE BOUNDARY LAYER

Experimental Details

The experimental setup for the laboratory model of the atmospheric convective boundary layer (cbl) has been described by Hibberd and Sawford (1989). The salient features of the experiment for this study are: (i) it is conducted in a 3.2mx1.6mx0.8m deep tank using saline solutions with typical convective velocities $w^* \approx$ 1cm/s; (ii) the mean depth of the convecting (or mixed) layer $z_i \approx$ 25cm; (iii) it includes penetrative entrainment at the top of the layer; (iv) the results are non-dimensionalized with w^* and z_i , and (v) the turbulence is homogeneous in the x and y-directions so that averaging can be carried out in horizontal planes.

The flow was seeded with 0.35-0.8mm diameter polystyrene beads with densities of 1.02g/cm^3 matched to the mixed layer density at the time of the experiment to ensure neutral buoyancy. The seeding density was approximately 0.1cm^{-3}. Illumination was provided from 2kW slit light sources, which were located at each end of the tank, and produced a white light sheet about 2cm wide through the length of the tank. This resolved motion in the x and z-directions. A Panasonic WV-CL502 CCD video camera with sensitivity

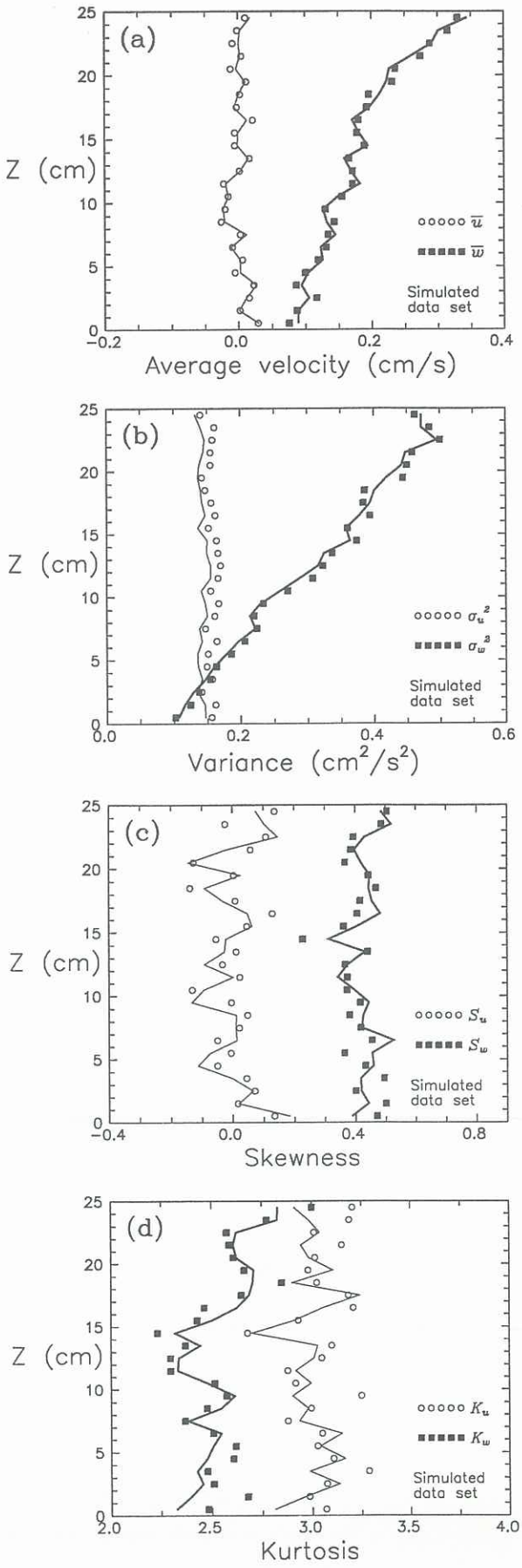

Fig. 2 Simulated test data; ——— *true* results from full data set; o, ■ particle tracking results.

of 10lux and equipped with an f1.2/12.5-75mm zoom lens was used to capture the images from a 60cmx40cm field of view of the tank. These were recorded on a Sony VO-5800PS U-matic video recorder.

Results

Approximately 5000 frames sampled at 5Hz from video recordings of several experiments were analyzed. This produced about 5000 velocity samples at each z-level. Figs. 3(a)-(c) show the resulting vertical profiles of the normalized variance, skewness and kurtosis of the vertical velocity fluctuations from analysis of these tracked data (■) and compare them with other data. The laboratory results of Adrian *et al* (1986) were obtained with a laser-doppler anemometer in a setup with no penetrative entrainment (lid at $z = z_i$) and hence diverge from the other data at higher z/z_i. The large scatter in the field data, obtained from aircraft traverses, results from the small sampling time for each measurement compared with the relevant timescale of about 10min for atmospheric convection.

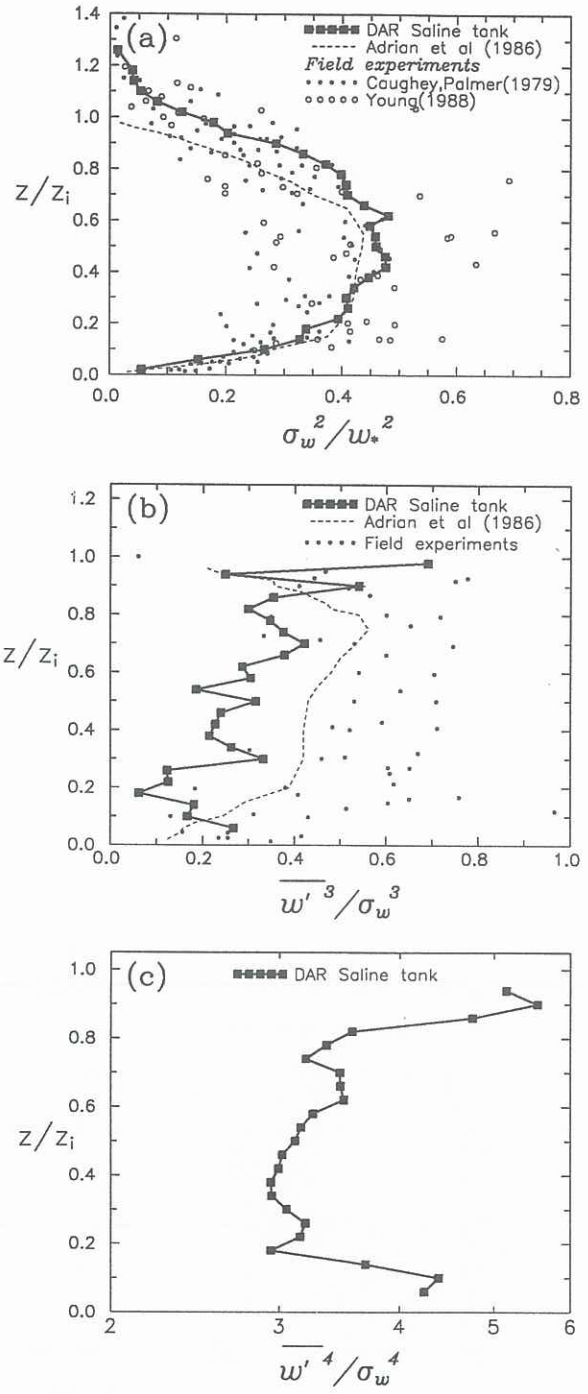

Fig. 3 Vertical profiles of central moments of the vertical velocity fluctuations from tracked data (■): (a) variance; (b) skewness, field data from Caughey and Palmer (1979), LeMone (1989); (c) kurtosis.

The variances from the saline tank show very little spread and good agreement with the other data, whereas the skewness results are noisier and somewhat lower. The positive skewness of w' is a result of the narrower and more intense thermals than downdraughts in the cbl. The kurtosis is seen to be close to 3 through a large part of the cbl, increasing towards the bottom and top of the layer, indicating a relatively greater spread of velocities than for a Gaussian distribution.

CONCLUSIONS

A particle tracking algorithm suitable for analysis of relatively low speed laboratory flows has been described. It relies on particle location data from video recordings and a frame-grabbing data acquisition system. It features the ability to track many particles over many sequential frames. This enables the technique to accurately follow particles with a wide range of velocities in a single experiment and avoids problems of directional ambiguity. A simulated set of trajectories has been used to check the operation of the algorithm. It has been demonstrated that accurate measurements of turbulence statistics can be obtained from the analysis of velocities from the particle tracking algorithm.

ACKNOWLEDGEMENTS

This work would not have been possible without the initial software development of the data acquisition and analysis systems by Mark Durre, as well as significant improvements in the implementation of the tracking algorithm made by Henry Granek, and testing of the technique on a variety of flows by Dave Murray. The assistance of George Scott in running the saline tank experiments is much appreciated.

REFERENCES

ADRIAN, RJ, FERREIRA, RTDS and BOBERG, T (1986) Turbulent thermal convection in wide horizontal fluid layers. *Experiments in Fluids* **4**, 121-141.

ADRIAN, RJ (1991) Particle-imaging techniques for experimental fluid mechanics. *Ann. Rev. Fluid Mech.* **23**, 261-304.

CAUGHEY, SJ and PALMER, SG (1979) Some aspects of turbulence structure through the depth of the convective boundary layer. *Quart. J. R. Met. Soc.* **105**, 811-827.

HESSELINK, L (1988) Digital image processing in flow visualization. *Ann. Rev. Fluid Mech.* **20**, 421-85.

HIBBERD, MF and SAWFORD, BL (1989) A laboratory model of convection in the atmospheric boundary layer, *Proc. 10th Australasian Fluid Mech. Conf. II*, Melbourne, 14.17-14.20.

HURLEY, PJ and PHYSICK, WL (1992) A skewed, homogeneous Lagrangian particle model for convective conditions. *Atmos. Environ.* (in press).

LeMONE, MA (1989) Some observations of vertical velocity skewness in the convective boundary layer, *J. Atmos. Sci.* **47**, 1163-1169.

YOUNG, GS (1988) Turbulence structure of the convective boundary layer, Part I: Variability of normalized turbulence statistics. *J. Atmos. Sci.* **45**, 719-26.